Supplementary information: *In situ* single particle characterization of the themoresponsive and co-nonsolvent behavior of PNIPAM microgels and silica@PNIPAM core-shell colloids

Albert Grau-Carbonell[1,*], Fabian Hagemans[1], Maarten Bransen[1], Nina A. Elbers[1], Relinde JA van Dijk-Moes[1], Sina Sadighikia[1], Tom A.J. Welling[1], Alfons van Blaaderen[1,*], and Marijn A. van Huis[1,*]

[1]Soft Condensed Matter, Debye Institute for Nanomaterials Science, Utrecht University, Princetonplein 1, Utrecht 3584 CC, The Netherlands
[*]Corresponding authors: A.vanBlaaderen@uu.nl, M.A.vanHuis@uu.nl, A.GrauCarbonell@gmail.com

1 Altering the composition of the solvent water

The contrast contribution of the solvent to a (S)TEM signal depends on the elemental composition and density of the liquid, as well as the thickness of the liquid layer. Thicker liquid layers will result in a higher scattering contribution of the solvent to the overall signal. The cell thickness is determined by the cell assembly conditions and optimized to fit the microgels, changing the elemental composition of the solution appears to be the most straightforward route. Importantly, the liquid medium should stay as chemically close as possible to pure water as the thermoresponsive behavior is known to sensitively depend on the solvent conditions. Here we report the results of dissolving salts consisting of medium-sized metal ions (Cu, from Tetrakis(acetonitrile)copper(I) hexafluorophosphate, 50 mM) to heavy metal ions (U, from Uranyl acetate, 5 mM) in water media in an attempt to increase the contrast of the solvent compared to that of the polymer. Our results show that following the known behavior of ions in water under electron beam illumination, solid particles from Cu (Figure S1A, SI Video 1) and a solid coating from U happened during LC-EM imaging (Figure S1B, SI Video 2). Interestingly, a strong oxigen signal was detected in such structures. U coating was more prevalent at the microgel parts further away from the windows (Supplementary Figure S4). PNIPAM microgels appeared to be a preferred substrate for the nucleation of these structures. Interestingly, nucleation happened at the outside of the more dense part of the microgels, pointing towards an increase in the concentration of nucleation points. Another possibility is that the shrinkage of the corona happened rapidly, before any observable metal deposition could happen. The chemistry in this process can be understood by combining the current knowledge of the reduction of metal ions and the formation of polymer macro-radicals by electron beam induced radiolysis species.[1, 2, 3] Metal ions are reduced to metal NPs by $H^{\cdot}$ and $e^{-}_{(aq)}$, which in turn are created in the radiolysis/interactions of the beam with the water. Metal particles with strong attractive van der Waals forces can have an affinity for the polymer chains and even charged particles can also follow the same fate, especially if polymers also harbor dangling electrons and/or if the radiolysis increases the ionic strength locally. At the same time metal ions can react with the charged chains and act as nuclei for the deposition of more metal. Therefore, because the extensive nature of the interaction between water radiolysis products and metal ions in solution, the dissolution of salts to increase solvent contrast does not appear to be suitable to study PNIPAM microgels in LC-EM studies. Furthermore, although some radical scavengers have shown the ability to minimize or even stop the reduction of metal ions from metal salts under electron beam illumination, we were not able to determine the position of the microgels before metal reduction started and therefore we believe that this strategy does not work for reasonable concentrations of salts.

Therefore, a simple and straightforward way to disperse metal atoms in media avoiding the reduction of new metal NPs in a liquid sample is to use already reduced metals. We approached this route by dispersing a number of NPs in our system. Silica, Au and Au@silica NPs are some of the most readily available and easy to synthesize colloidal systems, and we have shown in previous studies that they are stable under electron beam illumination in water for the low electron dose rates used in this study.[4] Gold was chosen because of its high atomic number and the ease to synthesize monodisperse NPs, being ligand-exchanged and/or coated by silica to disperse the Au NPs in water.[5, 6, 7] Unfortunately, electron beam-sample interactions hindered the applicability of this approach, since particle-particle, particle-window and particle-microgel attachments took place. These attachments were sometimes spontaneous and sometimes beam induced, depending on the dispersed NPs. These findings were however exploited into a successful procedure to image the PNIPAM by decorating the microgels as described in the next section.

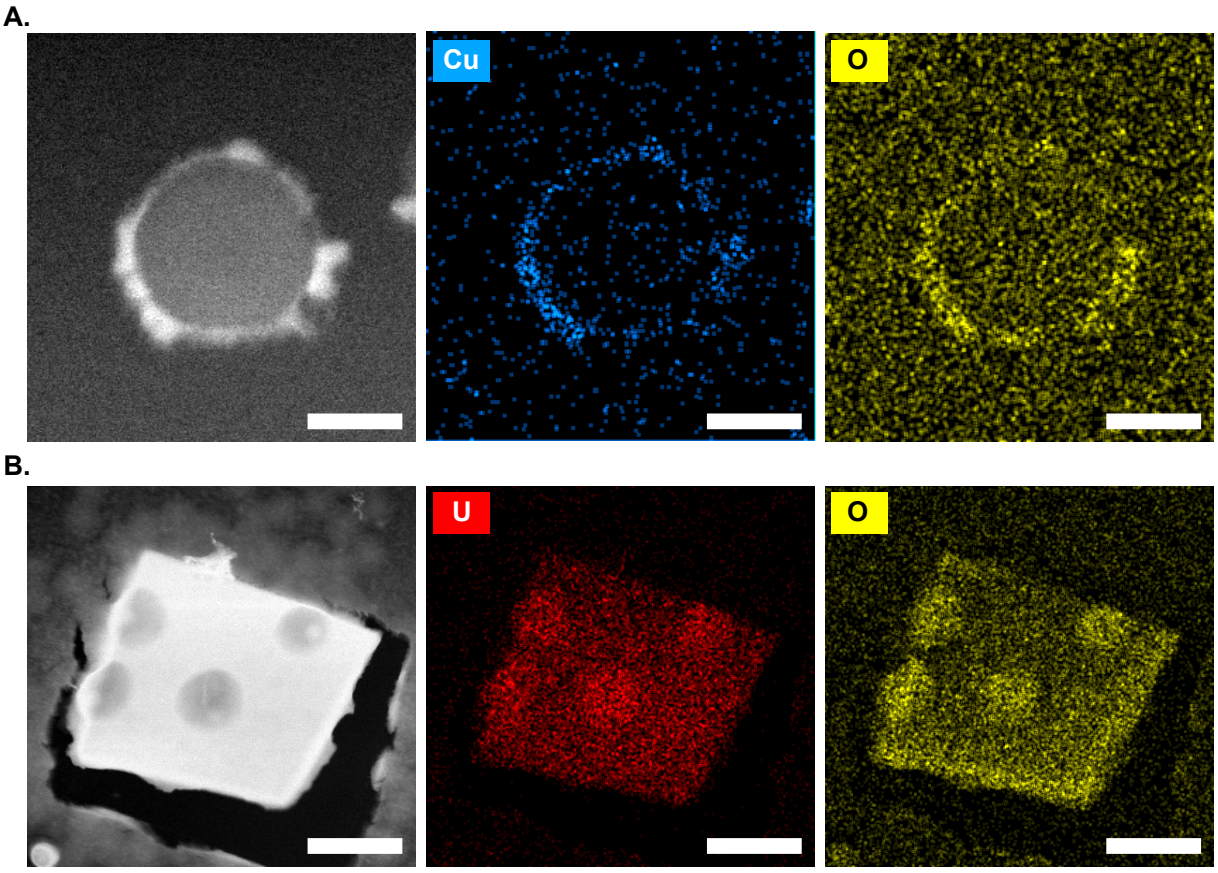

Figure S1: **Beam induced reduction of metal ions in solution onto PNIPAM microgels A.** Post-mortem HAADF-STEM imaging of the resulting PNIPAM covered by Cu NPs after the electron beam irradiation of microgels in water in the presence of Tetrakis(acetonitrile)copper(I) hexafluorophosphate (50 mM). Scale bars: 200 nm. **B.** Post-mortem HAADF-STEM imaging of the resulting PNIPAM covered by U NPs after the electron beam irradiation of microgels in water in the presence of Uranyl acetate (5 mM). Scale bars: 5 μm.

2 Decoration of microgels with high contrast marker NPs to resolve the low-contrast swollen PNIPAM microgels in water

Post-synthetic *in situ* labelling of PNIPAM microgels was the strategy that worked best to add contrast markers to the outer parts of the microgels. When high contrast NPs were attached to the outer parts of the low volume fraction corona, low electron dose rates could be used without the necessity to resolve the polymer itself. Various types of potential decorative NPs dispersed in water were flown into the liquid cell using the microfluidic capacity of our dedicated liquid cell holder and *in situ* measurements were subsequently performed.

All measurements of the total size of PNIPAM microgels made at RT (21 °C) with Au and SiO_2 NPs yielded particle sizes exceeding the previously measured size of 400 nm from bare PNIPAM microgels dispersed in water (**Table 1**). Silica particles showed efficient spontaneous attachment to PNIPAM but their contrast was low and bigger particles had to be used (113 ± 3 nm) which limited the accuracy of our measurements (Figure S2A). Citrate-stabilized gold NPs (D = 17 ± 1 nm) allowed easier measurements of the total particle size given their small size and high contrast, but their spontaneous attachment was not prevalent enough even at high particle concentrations, and had to be mediated by electron beam illumination (Figure S2B). We tailored the chemistry of the ligands on the citrate-stabilized gold NPs to try and change their interaction with the PNIPAM chains by covalently binding poly-etylene glycol molecules to the gold surface (Au-PEG NPs), with the PEG molecules functionalized in some cases with either amino (Au-PEG-NH_2 NPs) or acid (Au-PEG-COOH NPs) terminations. The Au-PEG NPs attached to PNIPAM NPs upon electron beam illumination (Figure S2C). The attachment took place only in the imaging area. If a particle fell partially inside the imaging area and partially outside, an uneven attachment of NPs happened. The Au-PEG-COOH NPs also attached to PNIPAM microgels upon electron beam illumination but started forming branched structures of NPs (Figure S2D, SI Video 3). The microgel size could only be measured after at least 1 frame and the measured particle size was smaller than D_{RT} (D_{RT} = 650-670 nm, RT = 21 °C). The Au-PEG-COOH NPs permanently attached to each other with small (1-2 nm) interparticle distances (Supplementary Figure S5), pointing to possible ligand-ligand crosslinking mediated by radiolysis radicals. Interestingly, Au-PEG-NH_2 showed a tendency towards spontaneously attaching to the cell windows but not to the PNIPAM microgels (Figure S2E). Upon imaging the Au-PEG-NH_2 the NPs slowly escaped the imaging area, most likely due to beam-induced charging of the NPs and the silicon nitride window (SI Video 4).

Because silica's high spontaneous attachment efficiency and small Au NP's ability to allow better measurements at low dose, we predicted that core-shell Au@SiO_2 NPs would combine the best of both systems. A combination of small Au cores with a thin silica coating with particle diameters of 17@39 ± 1@6 nm resulted in spontaneous decoration of the PNIPAM microgels and showed to be good marker particles to label PNIPAM swollen microgels including the low density outer corona's (Figure S2F) nm). The full size of the microgel corona decorated with Au@SiO_2 NPs could be precisely resolved despite the low polymer volume fraction (Figure S2D).

Table 1: Overview of sizes and results obtained for PNIPAM microgels at room temperature (21 °C) when decorated with marker NPs.

NP type	NP diameter (nm)	Type of attachment	Microgel diameter (nm)
SiO_2	113 ± 3	Spontaneous	500-550
Au-Citrate	17 ± 1	Beam Induced	500-550
Au-PEG	17 ± 1	Beam Induced	500-550
AuNP-PEG-COOH	17 ± 1	Beam Induced	500-550
AuNP-PEG-NH_2	17 ± 1	Spontaneous	Attachment to Si_xN_y window
AuNP@SiO_2	**17@39 ± 1@6**	**Spontaneous**	**670 ± 40**

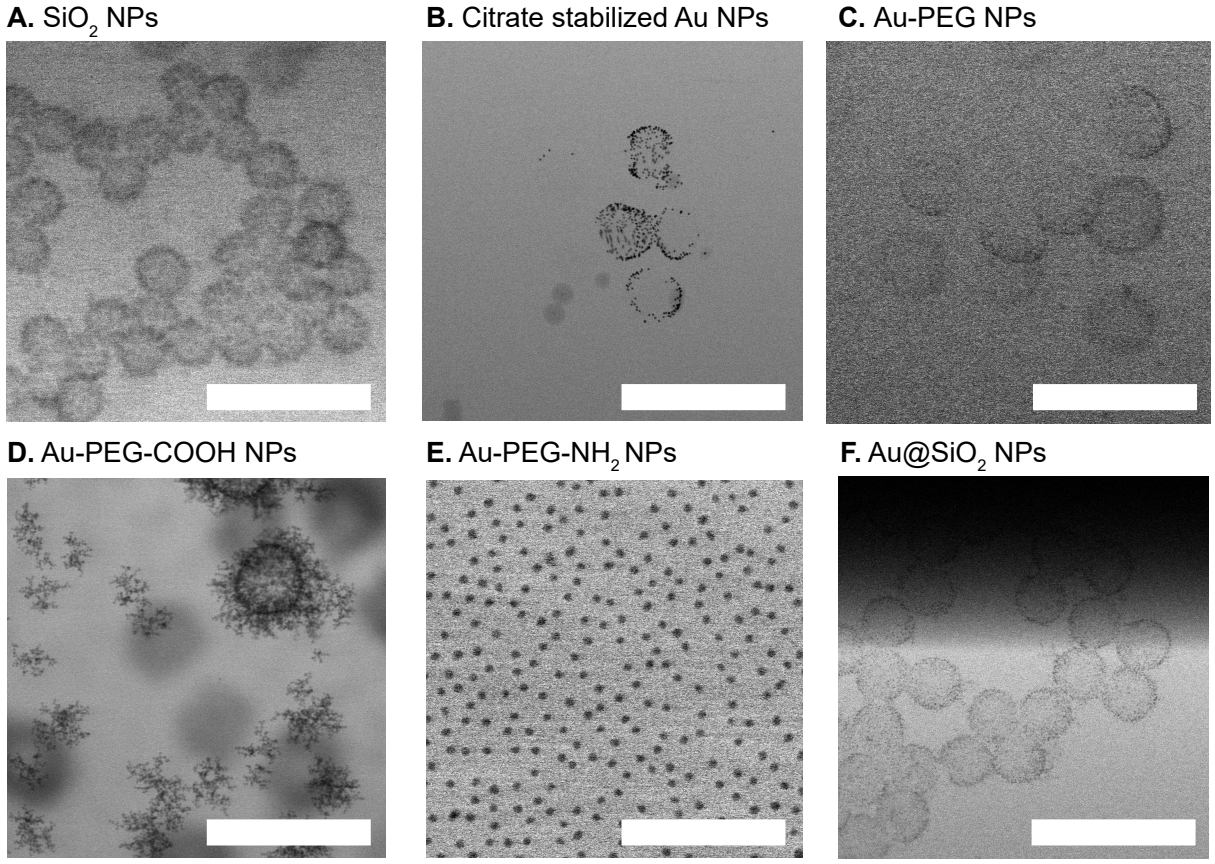

Figure S2: **Decoration of PNIPAM microgels with SiO_2, Au and Au@SiO_2 NPs A.** Spontaneous decoration with SiO_2 NPs (D = 113 ± 3 nm). Scale bar: 2 μm.**B.** Beam-induced decoration with citate stabilized Au NPs (D = 17 ± 1 nm). Scale bar: 1.5 μm. **C.** Beam-induced decoration with citate stabilized Au-PEG NPs (D = 17 ± 1 nm). Scale bar: 2 μm.**D.** Beam-induced decoration with citate stabilized Au-PEG-COOH NPs (D = 17 ± 1 nm). Scale bar: 1.5 μm. **E.** Au-PEG-NH_2 NPs (D = 17 ± 1 nm) attached to the silicon nitide window of the LC. Scale bar: 500 nm. **F.** Spontaneous decoration with Au@SiO_2 NPs (17@39 ± 1@6 nm). Scale bar: 3 μm.

3 Au@SiO_2 marker particles on SiO_2 spheres (Dry)

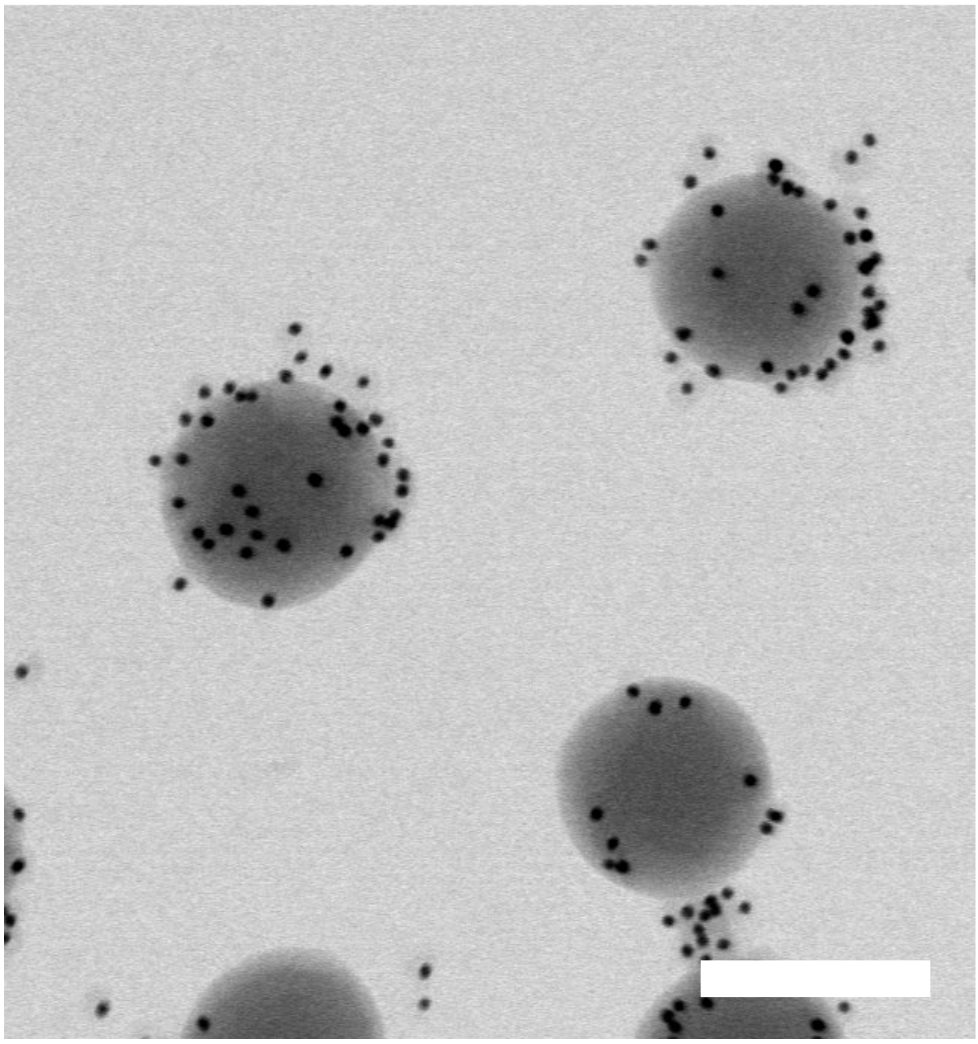

Figure S3: Sample of Au@SiO_2 marker NP dryed together with SiO_2. As marker NP rest on the SiO_2 it is readily seen that for hard particles the distance measured between the gold cores is slightly above the real size of the NP due to the presence of the SiO_2 shells. SiO_2 shells seen in this image are effectively invisible in water for all our imaging conditions. Scale bar: 500 nm.

4 Beam-induced metal deposition in solution from an Uranyl acetate solution

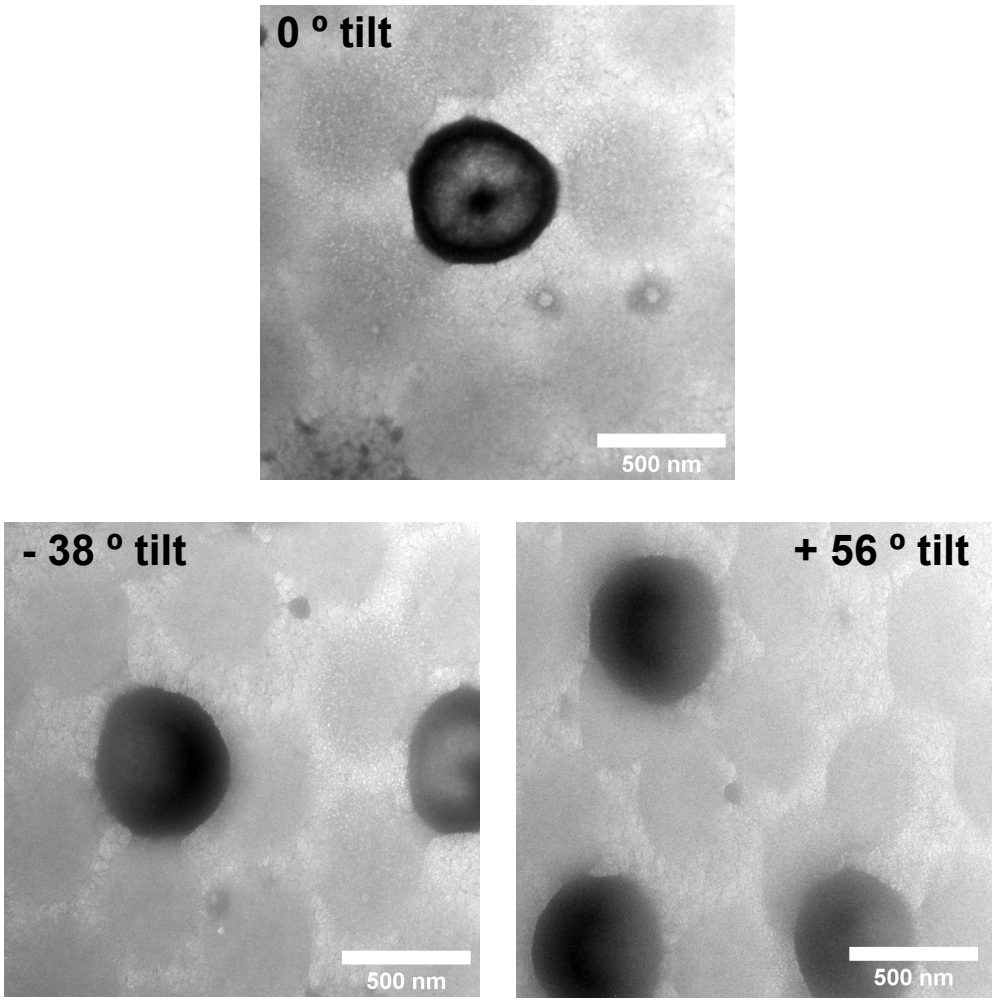

Figure S4: **A.** Post-mortem (dry) (S)TEM image of an area covered with several PNIPAM microgels imaged in an uranyl acetate aqueous solution (0.2 w/w %) and its surroundings. A solid layer reduced from the metal ions in solution. The microgels in this layer appear with a lower contrast due to the lower electron density of their volume due to the polymer compared to the purely precipitated surrounding. **B.** Post-mortem (dry) top view of a PNIPAM microgel imaged in the same uranyl acetate aqueous solution. Metal ions reduced preferentially in the particle regions directly exposed to the solvent as can be observed if the sample is tilted, as seen in **C.** and **D.**. Scale bars: 500 nm.

5 Beam-induced Au NPs attachment

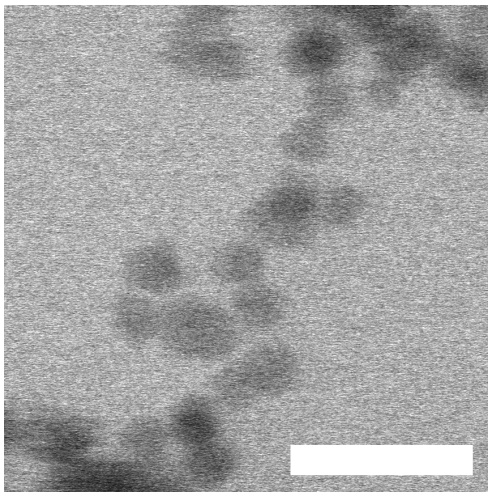

Figure S5: Au-PEG-COOH gold NPs irreversibly attached due to electron beam illumination of a dispersion of such NPs in water. Assembly in this case happened on the silicon nitride window of a liquid cell. Between some particles a minimal spacing can be seen, indicating that their surfaces are not necessarily attached. A possible interpretation for this is that the attachment is mediated by the ligands on the NP surface. Scale bar: 100 nm.

6 Anisotropic beam-effects on PNIPAM microgels

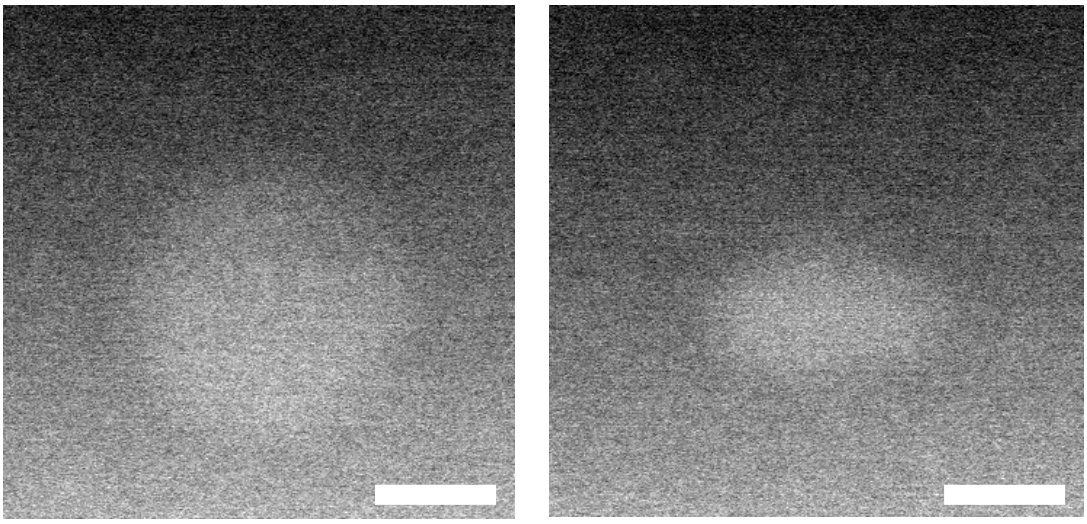

Figure S6: PNIPAM microgel imaged at a high electron dose rate (920 $e^{-}nm^{-2}s^{-1}$). The microgel became elongated in the scanning direction of the electron beam. Scale bars: 150 nm.

Videos

Supplementary videos can be downloaded free of charge from:
https://drive.google.com/drive/folders/1ZnDsAiwgq5yOy3ReZG0dfuSRlX-JbKXm?usp=sharing

References

[1] T. J. Woehl, J. E. Evans, I. Arslan, W. D. Ristenpart, and N. D. Browning. Direct in situ determination of the mechanisms controlling nanoparticle nucleation and growth. *ACS Nano*, 6(10):8599–8610, 2012.

[2] A.A. Zezin, D.I. Klimov, E.A. Zezina, K.V. Mkrtchyan, and V.I. Feldman. Controlled radiation-chemical synthesis of metal polymer nanocomposites in the films of interpolyelectrolyte complexes: Principles, prospects and implications. *Radiat. Phys. Chem.*, 169:108076, 2020.

[3] A. Ashffag, J. An, P. Ulanski, and A. Mohamad. On the mechanism and kinetics of synthesizing polymer nanogels by ionizing radiation-induced intramolecular crosslinking of macromolecules. *Pharmaceutics*, 13(11):1765, 2021.

[4] A. Grau-Carbonell, S. Sadighikia, T.A.J. Welling, R.J.A. van Dijk-Moes, R. Kotni, M. Bransen, A. van Blaaderen, and M.A. van Huis. *In situ* study of the wet chemical etching of SiO_2 and nanoparticle@SiO_2 coreshell nanospheres. *ACS Appl. NanoMater.*, 4(2):1136–1148, 2021.

[5] C. Graf, D. L. J. Vossen, A. Imhof, and A. van Blaaderen. A general method to coat colloidal particles with silica. *Langmuir*, 19:6693–6700, 2003.

[6] P. del Pino, F. Yang, B. Pelaz, Q. Zhang, K. Kantner, R. Hartmann, N. Martinez de Baroja, M. Gallego, M. Möller, B.B. Manshian, S.J. Soenen, R. Riedel, N. Hampp, and W.J. Parak. Basic physicochemical properties of polyethylene glycol coated gold nanoparticles that determine their interaction with cells. *Angew. Chem. Int. Ed.*, 55(18):5483–5487, 2016.

[7] J. Fokkema, J. Fermie, N. Liv, D.J. van den Heuvel, T.O.M. Konings, G.A. Blab, A. Meijerink, J. Klumperman, and H.C. Gerritsen. Fluorescently labelled silica coated gold nanoparticles as fiducial markers for correlative light and electron microscopy. *Sci. Rep.*, 8:13625, 2018.